

# A pulsating regime of magnetic deflagration

M. Modestov, V. Bychkov, M. Marklund

*Department of Physics, Umeå University, SE-901 87 Umeå, Sweden*

The stability of a magnetic deflagration front in a collection of molecular magnets, such as  $\text{Mn}_{12}$ -acetate, is considered. It is demonstrated that stationary deflagration is unstable with respect to one-dimensional perturbations if the energy barrier of the magnets is sufficiently high in comparison with the release of Zeeman energy at the front; their ratio may be interpreted as an analogue to the Zeldovich number, as found in problems of combustion. When the Zeldovich number exceeds a certain critical value, a stationary deflagration front becomes unstable and propagates in a pulsating regime. Analytical estimates for the critical Zeldovich number are obtained. The linear stage of the instability is investigated numerically by solving the eigenvalue problem. The nonlinear stage is studied using direct numerical simulations. The parameter domain required for experimental observations of the pulsating regime is discussed.

## I. INTRODUCTION

Molecular magnets have been a subject of intense experimental and theoretical studies for almost two decades, see Refs. [1,2] for a review. The field belongs to mesoscopic physics as the typical length scales are between micro- and macroscopic. Such an intermediate parameter regime provides unique conditions for observing quantum and classical phenomena acting together. Besides, a large magnetic spin of a single molecule makes molecular magnets natural candidates for novel magnetic storage media and quantum computing<sup>3,4</sup>.

Two prominent and well investigated materials in this research field are  $\text{Mn}_{12}$ -acetate and  $\text{Fe}_8$ , both which demonstrate super-paramagnetic properties<sup>1</sup>. They both have a large spin at the ground state ( $S = 10$ ) and strong magnetic anisotropy with 10 pairs of degenerated levels corresponding to positive and negative projections  $S_z$  on a chosen axis, and an additional level with  $S_z = 0$ <sup>5-8</sup>. When an external magnetic field is applied to a sample of molecular magnets along the crystal axis, then spin orientation in the direction of the field becomes preferable. At low temperature all molecules populate only one level (e.g.  $S_z = 10$ ) and the magnetization reaches the saturation value. If the direction of the external magnetic field changes to the opposite one, then the former ground state of the molecules becomes metastable with an increased potential energy (the Zeeman energy). An energy barrier hinders direct transition of the molecules from the metastable state to the new ground state, which, therefore, can occur as a thermal relaxation or as avalanches. Thermal relaxation goes slowly and uniformly in space for the whole sample. At temperatures of a few Kelvin this process may be neglected, since its characteristic time is rather large, e.g., about two months for  $\text{Mn}_{12}$  at 2 K<sup>5</sup>. However, many experimental works on molecular magnets demonstrated quite fast transition in a form of avalanche with the characteristic time about few milliseconds<sup>9,10</sup>. Recent detailed studies of the avalanche revealed that the spin reversal does not happen simultaneously within the whole sample in that case, but it occurs in a narrow zone propagating as a front at a velocity of several meters per second<sup>11-18</sup>. The avalanche is accompanied by significant heat release similar to a deflagration wave in combustion and for this reason it was named “magnetic deflagration”.

In slow combustion, the deflagration front corresponds to a thin zone of chemical reactions separating the cold fuel mixture and the hot burned products<sup>19</sup>. The released energy is transmitted to the cold fuel mixture due to thermal conduction; the temperature of the fuel mixture increases, which stimulates chemical reactions. The slow combustion front propagates in gaseous mixtures with a substantially subsonic velocity within the range from several centimeters to several meters per second<sup>19</sup>. Analogously, in magnetic deflagration, the energy of chemical reactions is replaced by the Zeeman energy of the molecular magnets in an external magnetic field. The released energy is distributed to the neighboring layers by thermal conduction, which increases the temperature of the originally cold medium and leads to much higher probability of spin transition. In recent studies, Garanin and Chudnovsky<sup>12</sup> developed a theoretical description of a planar stationary magnetic deflagration with maximal possible release of the Zeeman energy (they called such a regime “full burning”). Since then, a number of papers have been devoted to ignition techniques and speed measurements of the magnetic deflagration in  $\text{Mn}_{12}$ <sup>14-18</sup>. Magnetic avalanches have been also observed in other materials, like the intermetallic compound  $\text{Gd}_5\text{Ge}_4$ <sup>20</sup>. However, the magnetic “burning” does not necessarily have to be complete. As we show in the present paper, the Zeeman energy release depends on the external magnetic field and on the initial concentration of active molecules. A sufficiently low energy release may lead to a new pulsating regime of magnetic deflagration.

The aim of the present work is to study the stability of a planar stationary front of magnetic deflagration. Here, we demonstrate that stationary deflagration is unstable with respect to one-dimensional perturbations if the Zeeman energy release at the front is sufficiently low in comparison with the energy barrier of the spin transition. The condition of the instability may be formulated using the Zeldovich number, similar to the case of combustion of solid propellants<sup>19,21-25</sup>. In the problem of magnetic deflagration, the Zeldovich number is essentially given by the ratio of the energy barrier of the molecular magnets and the temperature at the deflagration as determined by the Zeeman energy release. When the Zeldovich number exceeds a certain critical value, a stationary deflagration front becomes unstable and propagates in a pulsating regime. We obtain analytical estimates for the critical

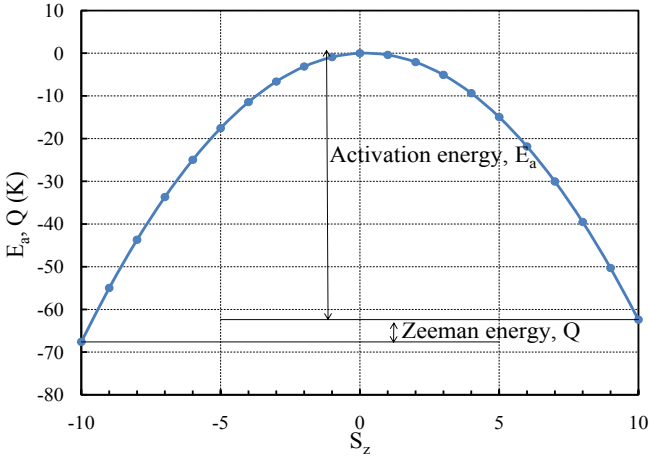


FIG. 1: The energy levels for the magnetic molecule system of  $\text{Mn}_{12}$  in the external magnetic field  $H_z = 0.2T$

Zeldovich number. We investigate the linear stage of the instability numerically by solving the eigenvalue problem. We study the nonlinear stage using direct numerical simulations. We also discuss the experimental parameters required for observations of the pulsating regime.

## II. A PLANAR STATIONARY FRONT WITH INCOMPLETE ZEEMAN ENERGY RELEASE

We consider a system of molecular magnets placed in an external magnetic field taking  $\text{Mn}_{12}$ -acetate as a particular example. The simplified Hamiltonian of the system has been suggested to take the form<sup>12</sup>

$$\mathcal{H} = -DS_z^2 - g\mu_B H_z S_z, \quad (1)$$

where  $S$  denotes the spin,  $D \approx 0.65K$  is the magnetic anisotropy constant,  $g \approx 1.94$  is the gyromagnetic factor,  $\mu_B$  is the Bohr magneton, and  $H_z$  is the external magnetic field. The energy levels for a molecule magnet  $\text{Mn}_{12}$  in the external field of  $H_z = 0.2T$  are depicted in Fig. 1. In Fig. 1 we indicate the Zeeman energy  $Q$  and the energy barrier  $E_a$  of the transition from the metastable state to the ground state, which plays the role of the activation energy for magnetic deflagration (both values are presented in temperature units). Using the Hamiltonian Eq. (1) we find how these two energies depend on the magnetic field, according to

$$E_a = DS_{10}^2 - g\mu_B H_z S_{10} + \frac{g^2}{4D} \mu_B^2 H_z^2 \quad (2)$$

and

$$Q = 2g\mu_B H_z S_z. \quad (3)$$

The last term in Eq. (2) is quite small as compared to the first two terms, so the activation energy decreases with increase of the magnetic field. However, the Zeeman energy increases linearly with the magnetic field. If the magnetic

field is high enough, the energy difference between the ground state ( $S_z = -10$ ) and the metastable state ( $S_z = 10$ ) is rather large, so that all the molecules tend to occupy the lowest energy level, i.e.  $S_z = -10$  in Fig. 1. When the direction of the external magnetic field switches to the opposite one, then the ground state and the metastable state exchange places and all the molecules tend to change their spin projection to the opposite one. Garanin and Chudnovsky identified such a transition as “full burning” of molecular magnets<sup>12</sup>. They also indicated that the regime of full burning is possible if the magnetic field is stronger than a certain critical value. Still, the external magnetic field is a controlled parameter of the experiments, which allows the possibility of incomplete burning in magnetic deflagration. We also point out that the analytical method used to calculate the magnetic deflagration speed in [12] is rigorous only in the limit of an activation energy large compared to the energy release, a condition which is satisfied to a much better degree in the regime of incomplete burning. In the present paper we are interested in the regime of incomplete burning in magnetic deflagration achieved for a sufficiently low external magnetic field. In that case the Zeeman energy is rather low, so that we obtain the fraction of molecules on the first energy level according to

$$n = \frac{1}{\exp(Q/T) + 1}, \quad (4)$$

where total number of molecules in all energy levels corresponds to unity. Still, in the typical experimental conditions, population of levels above the first one is negligible. At the same time, the fraction at the first level, Eq. (4), may be significant in a low magnetic field and cannot be neglected. As we will see, the stability of magnetic deflagration is sensitive to the activation energy scaled by the energy release in the process. This ratio increases also when the active  $\text{Mn}_{12}$  molecules are “diluted” with some neutral media as it was performed experimentally in, e.g., [26–28]. When mixed carefully with other compounds, the  $\text{Mn}_{12}$  molecules retain their magnetic properties. Since the heat release in magnetic deflagration happens only due to active magnet molecules, then the neutral compound reduces total energy release and the final temperature of the sample,  $T_f$ , thus increasing the scaled activation energy  $E_a/T_f$ . As a result, the scaled activation energy in magnetic deflagration becomes a free parameter, which may be controlled in the experiments by the external magnetic field and by the level of dilution.

The governing equations for magnetic deflagration are<sup>12</sup>

$$\frac{\partial E}{\partial t} = \nabla \cdot (\kappa \nabla E) - fQ \frac{\partial n}{\partial t}, \quad (5)$$

$$\frac{\partial n}{\partial t} = -\frac{1}{\tau_R} \exp\left(-\frac{E_a}{T}\right) \left[ n - \frac{1}{\exp(Q/T) + 1} \right] \quad (6)$$

where  $E$  is the thermal phonon energy,  $\kappa$  is thermal diffusion of energy,  $Q$  is the Zeeman energy release in temperature units,  $f \leq 1$  indicates possible reduction of the energy release because of dilution of active molecules ( $f = 1$  corresponds to zero dilution),  $n$  is fraction of magnetic molecules

in the metastable state,  $E_a$  is the energy barrier of tunneling measured in temperature units and  $\tau_R$  is a constant of time dimension. In magnetic deflagration, thermal diffusion and heat capacity depend strongly on temperature. Following<sup>12</sup>, we take the heat capacity in the classical form corresponding to phonons<sup>29</sup>

$$C = Ak_B \left( \frac{T}{\Theta_D} \right)^\alpha, \quad (7)$$

where  $\Theta_D$  is the Debye temperature, with  $\Theta_D = 38K$  for  $Mn_{12}$ ,  $k_B$  is the Boltzmann constant,  $A = 12\pi^4/5$  corresponds to the simple crystal model,  $\alpha$  is the problem dimension (we take  $\alpha = 3$  in most of the calculations, which corresponds to the 3D geometry). Dependence of thermal diffusion on temperature may be taken in the form  $\kappa \propto T^{-\beta}$ , where parameter  $\beta$  was considered in Refs. [12,30] within the range between 0 and 13/3. In the present paper we take  $\beta$  within the same range, and show that it has minor influence on the deflagration stability. Using the definition of heat capacity,  $C = dE/dT$ , we find the phonon energy as a function of temperature

$$E = \frac{Ak_B}{\alpha + 1} \left( \frac{T}{\Theta_D} \right)^\alpha T. \quad (8)$$

An important parameter of deflagration dynamics is determined by the ratio of the energy barrier (in temperature units) and the temperature in the hot region,  $E_a/T_f$ . A combustion counterpart of this value is related to the activation energy of chemical reaction, which is typically rather large. In the case of complete burning in magnetic deflagration of  $Mn_{12}$  this parameter was evaluated in [12] as  $E_a/T_f \approx 6$ , which is not a large value. At the same time, this parameter may increase almost without limits at low magnetic fields and for considerable dilution of active molecular magnets. When the ratio  $E_a/T_f$  is very large, the transition from the metastable to stable states goes in a thin region where the Arrhenius function in Eq. (6) is different from zero. In this limit we may obtain an analytical solution to Eqs. (5), (6) by the classical method of Zeldovich-Frank-Kamenetsky<sup>19</sup>, which was applied to magnetic deflagration in [12]. In a general case of finite  $E_a/T_f$ , the system Eqs. (6), (6) may be solved numerically as an eigenvalue problem.

First, we calculate the final temperature in the hot region behind the magnetic deflagration front. Using the energy conservation and Eqs. (4), (5), (8) we obtain

$$\frac{AT_0^{\alpha+1}}{fQ(\alpha+1)\Theta_D^\alpha} + 1 - \frac{1}{\exp(Q/T_0) + 1} = \frac{AT_f^{\alpha+1}}{fQ(\alpha+1)\Theta_D^\alpha} + \frac{1}{\exp(Q/T_f) + 1}. \quad (9)$$

Equation (9) determines the final temperature  $T_f$  as a function of the magnetic field, the dilution factor  $f$  and other parameters of the process. The first terms on both sides stand for the thermal energy, though initial thermal energy is usually rather small. The other terms indicate the fractions of molecules occupying the first energy level. In the case of full burning considered in [12] this equation becomes much simpler and may

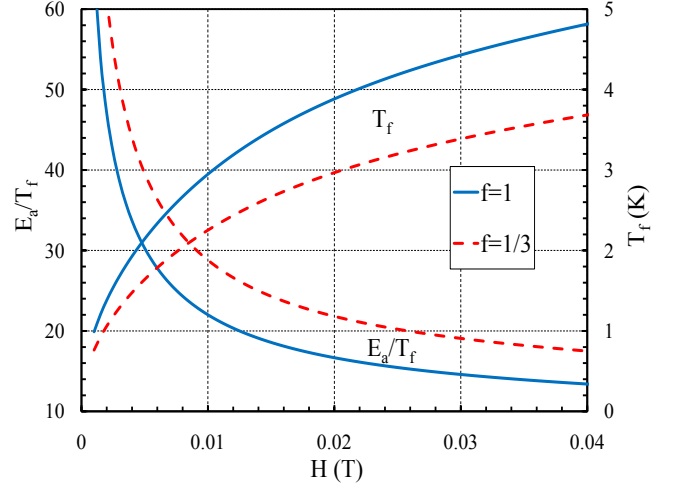


FIG. 2: The final temperature and the scaled activation energy in magnetic deflagration versus the magnetic field for the initial temperature  $T_0 = 0.2K$  and two dilution factors  $f = 1; 1/3$ .

be solved analytically. In the case of incomplete burning, a numerical solution to Eq. (9) is required. In Fig. 2 we show the numerical solution to Eq. (9), i.e. the final temperature and the scaled activation energy versus the magnetic field for two dilution factors  $f = 1; 1/3$ . In Fig. 2 we take the initial temperature  $T_0 = 0.2K$ , though it has minor influence on the result. The dilution factor  $f = 1$  stands for pure  $Mn_{12}$  media, while  $f = 1/3$  means that the average energy release is 3 times lower in comparison with the pure substance. The final temperature increases with the magnetic field, while the scaled activation energy decreases. The change in the scaled activation energy due to the dilution factor may be also quite strong.

We consider a stationary solution to Eqs. (5), (6) in the form of a planar front propagating with velocity  $U_f$ . To be particular, we assume that the front moves along the x-axis in the negative direction as shown in Fig. 3. Taking the reference frame of the front, we find

$$U_f \frac{d}{dx} (E + fQn) = \frac{d}{dx} \left( \kappa \frac{dE}{dx} \right), \quad (10)$$

$$U_f \frac{dn}{dx} = -\frac{n}{\tau_R} \exp\left(-\frac{E_a}{T}\right) \left[ n - \frac{1}{\exp(Q/T) + 1} \right]. \quad (11)$$

Integrating Eq. (10) from the initial to final states (labels 0 and f, respectively) and neglected the initial thermal energy, we obtain the final energy as

$$E_f = fQ(n_0 - n_f). \quad (12)$$

Integral to Eq. (10) specifies the internal structure of the transition zone

$$U_f fQ(n_0 - n_f) = \kappa_f \frac{dE}{dx}. \quad (13)$$

In the limit of a large activation energy,  $E_a/T_f \gg 1$ , the transition region may be presented as a surface of weak discontinuity, where energy and temperature are continuous and tend to their maximal values  $E \rightarrow E_f$ ,  $T \rightarrow T_f(E_f)$ , while their derivatives experience jump. In this limit one obtains the magnetic deflagration velocity<sup>19</sup>

$$U_f = \sqrt{\frac{\kappa_f}{Z\tau_R}} \exp\left(-\frac{E_a}{2T_f}\right), \quad (14)$$

where

$$Z = \frac{E_a f Q (n_f - n_0)}{T_f C_f T_f} = \frac{1}{(\alpha + 1)} \frac{E_a}{T_f} \quad (15)$$

plays the role of the Zeldovich number; the last relation in Eq. (15) follows from Eqs. (7), (8) and (12). Equation (14) for the deflagration velocity coincides with Eq. (109) in Ref. [12]. With the accuracy of a factor of  $1/(\alpha + 1)$ , the Zeldovich number shows the ratio of the activation energy and the final temperature in the deflagration front. Strictly speaking, the approach of a thin transition zone holds as long as Zeldovich number is large  $Z \gg 1$ , which is not applicable to the regime of full burning. We can find the dependence of the Zeldovich number upon the main experimental parameters of the problem taking into account Eqs. (2),(3),(7),(8) and (12)

$$Z = \left[ \frac{A}{2(\alpha + 1)^{\alpha+2} \Theta_D^\alpha g \mu_B S_z H_z f (n_0 - n_f)} \right]^{\frac{1}{\alpha+1}} \times \left( DS_{10}^2 - g \mu_B H_z S_{10} + \frac{g^2}{4D} \mu_B^2 H_z^2 \right). \quad (16)$$

Equation (16) shows how the Zeldovich number depends on the magnetic field and the dilution factor. In particular, high values of the Zeldovich number correspond to the low field strength. For a simplified quantitative estimate one can neglect the magnetic terms in the second couple of parentheses, which provide a contribution less than few percents for fields about 0.1 T and smaller, and find an evaluation for the Zeldovich number

$$Z \approx 1.3 [H_z f (n_0 - n_f)]^{-1/4}, \quad (17)$$

where  $H_z$  is the magnetic field in tesla.

### III. ANALYTICAL ESTIMATES FOR THE PULSATION INSTABILITY

In this section we obtain an analytical scaling for the 1D instability of the magnetic deflagration front in the model of a thin transition zone, i.e. at a large Zeldovich number  $Z \gg 1$ . In that case, according to Eq. (14), the deflagration velocity is extremely sensitive to temperature variations in the transition zone. In comparison with the Arrhenius function  $\exp(-E_a/2T_f)$ , all other parameters in Eq. (14) may be treated as constant. Temperature in the transition zone may

vary because of the front perturbations, and the instant front velocity may be written as

$$U_t = U_f \exp\left(\frac{E_a}{2T_f} - \frac{E_a}{2T_t}\right), \quad (18)$$

where label  $f$  refers to the stationary case, whilst  $t$  indicates the time-dependent temperature in the infinitely thin transition zone. Position of the transition zone,  $x = \phi(t)$ , in the stationary reference frame is determined by the equation

$$\frac{\partial \phi}{\partial t} = -U_f \left[ \exp\left(\frac{E_a}{2T_f} - \frac{E_a}{2T_t}\right) - 1 \right], \quad (19)$$

where the first minus sign indicates propagation of the front in the negative direction. Boundary conditions at the transition region may be found similar to<sup>19,22</sup>. Integrating Eq. (5) twice over the transitional zone, we obtain continuous energy and temperature

$$E_{\phi+} = E_{\phi-}, \quad (20)$$

where the labels  $\phi_{\pm}$  correspond to hot and cold sides of the transition zone. The first derivative of energy (i.e. energy flux) experiences jump at the interface as

$$-U_f Q n_0 \exp\left(\frac{E_a}{2T_f} - \frac{E_a}{2T_t}\right) = \kappa_f \left( \frac{\partial E}{\partial x} \right)_{\phi+} - \kappa_f \left( \frac{\partial E}{\partial x} \right)_{\phi-}. \quad (21)$$

We investigate the linear stability of the stationary deflagration and consider small perturbations of all variables in the exponential form  $\tilde{E} \propto \exp(\sigma t)$ , where the growth rate  $\sigma$  may have both real and imaginary parts. We solve the stability problem analytically in the limit of a thin transition zone similar to [19]. Outside the transition zone the perturbed equations (5)-(6) are

$$\sigma \tilde{E} + U_f \frac{\partial \tilde{E}}{\partial x} = \frac{\partial^2}{\partial x^2} (\kappa \tilde{E}), \quad (22)$$

$$\sigma \tilde{n} + U_f \frac{\partial \tilde{n}}{\partial x} = 0. \quad (23)$$

Behind the transition zone we have  $\tilde{n} = 0$ . Similar to the respective combustion problem<sup>19</sup>, we consider first a hypothetical case of constant coefficient of thermal conduction  $\kappa = \text{const} = \kappa_f$ . Solving Eq. (22) outside the transition zone with  $\tilde{E} \propto \exp(\mu x)$  we find two modes

$$\mu^2 - \frac{U_f}{\kappa_f} \mu - \frac{\sigma}{\kappa_f} = 0, \quad (24)$$

$$\mu_{0,1} = \frac{U_f}{2\kappa_f} \pm \sqrt{\frac{U_f^2}{4\kappa_f^2} + \frac{\sigma}{\kappa_f}}, \quad (25)$$

with labels 0 and 1 indicating media ahead and behind the transition zone. In the case of magnetic deflagration, thermal conduction decreases strongly with temperature,  $\kappa \propto T^{-\beta}$ . Still, the mode behind the transition zone with  $\mu_1 < 0$  is an exact solution to the linearized Eq. (19) even in that case, since temperature behind the transition zone is uniform in the stationary deflagration. On the contrary, the mode ahead of the transition zone with  $\mu_0 > 0$  is only an approximation. Similar to the combustion theory<sup>19</sup>, we may define the parameter  $L_f \equiv \kappa_f/U_f$  as the deflagration front thickness related to thermal conduction in the hot region. At the same time, the characteristic length scale of temperature profile in the stationary deflagration increases in the cold layers as  $\kappa(T)/U_f$ , which allows to consider them as quasi-uniform with respect to the perturbations. Indeed, the mode ahead of the transition zone describes decay of perturbations at the length scale  $\mu_0^{-1}$  with

$$\mu_0 = \frac{1}{2L_f} \left[ 1 + \sqrt{1 + 4\sigma L_f/U_f} \right] \propto \frac{1}{L_f}. \quad (26)$$

Therefore, investigating the 1D instability analytically, it is justified to consider only the heating layer of the size about  $L_f$  close to the transition zone and to treat the coefficient of thermal conduction as approximately constant. The numerical solution to the problem obtained below supports the analytical approximation.

We consider perturbations of the boundary conditions (19) – (21) at the transition surface

$$\sigma\phi = -U_f \frac{E_a}{2C_f T_f^2} \tilde{E}_{\phi+}, \quad (27)$$

$$\tilde{E}_{\phi+} = \tilde{E}_{\phi-} + \phi \left( \frac{dE}{dx} \right)_{\phi-} = \tilde{E}_{\phi-} + \phi n_0 Q/L_f. \quad (28)$$

$$\begin{aligned} -U_f Q n_0 \frac{E_a}{2C_f T_f^2} \tilde{E}_{\phi+} &= \kappa_f \left( \frac{\partial \tilde{E}}{\partial x} \right)_{\phi+} - \kappa_f \left( \frac{\partial \tilde{E}}{\partial x} \right)_{\phi-} \\ &\quad - \kappa_f \phi \left( \frac{\partial^2 E}{\partial x^2} \right)_{\phi-}. \end{aligned} \quad (29)$$

The last equation may be also modified as

$$-Q n_0 \frac{E_a}{2C_f T_f^2} \tilde{E}_{\phi+} = \mu_1 L_f \tilde{E}_{\phi+} - \mu_0 L_f \tilde{E}_{\phi-} - \phi n_0 \frac{Q}{L_f} \quad (30)$$

taking into account the perturbation modes. Thus, we have to solve the algebraic system of three equations (27), (28) and (30), taking into account the modes (25). After heavy but straightforward algebra we end up with a simple quadratic equation

$$\left( \frac{4\sigma L}{U_f} \right)^2 - \frac{4\sigma L}{U_f} (Z^2/4 - 2Z - 1) + 2Z = 0, \quad (31)$$

which is similar to the respective result in the combustion theory<sup>19</sup>. Equation (31) describes the instability growth rate

as a function of the Zeldovich number. According to Eq. (31), the instability develops for  $Z > 4 + 2\sqrt{5} \approx 8.5$ . Close to this critical value the real part of the growth rate  $\text{Re}\sigma$  goes to zero, while the imaginary part remains finite,  $\omega = \text{Im}\sigma \neq 0$ , which indicates the pulsation regime of the instability. The obtained critical value of the Zeldovich number corresponds to rather high scaled activation energy,  $E_a/T_f \approx 34$ , see Eq. (15), in comparison with the values typical for the regime of full burning Ref. [12]. Still, this value is attainable experimentally for smaller magnetic fields and some dilution of the active molecules. At even larger value of the Zeldovich number,  $Z = 11.7$ , corresponding to  $E_a/T_f = 46.8$ , Eq. (31) demonstrates bifurcation, so that the instability growth rate becomes purely real with zero imaginary part for  $Z > 11.7$ . Below we will compare the analytical scaling Eq. (31) to the numerical solution to the problem taking into account finite width of the transition zone.

#### IV. NUMERICAL SOLUTION TO THE STABILITY PROBLEM TAKING INTO ACCOUNT FINITE WIDTH OF THE TRANSITION ZONE

In this section we solve the stability problem numerically taking into account finite width of the transition zone. We introduce dimensionless variables and parameters

$$\theta = T/T_f, \quad a = n/n_0, \quad \xi = x/L_f,$$

$$\Theta = E_a/T_f, \quad \Delta = Q/T_f, \quad \kappa = \kappa_f \theta^{-\beta} \quad (32)$$

and rewrite the evolution equations (5)-(6) to

$$\begin{aligned} \theta^\alpha \frac{\partial \theta}{\partial \tau} + \theta^\alpha \frac{\partial \theta}{\partial \xi} &= \frac{\partial}{\partial \xi} \left( \theta^{\alpha-\beta} \frac{\partial \theta}{\partial \xi} \right) + \\ J \Lambda \exp \left( -\frac{\Theta}{\theta} \right) &\left[ a - \frac{1}{\exp(\Delta/\theta) + 1} \right], \end{aligned} \quad (33)$$

$$\frac{\partial a}{\partial \tau} + \frac{\partial a}{\partial \xi} = -\Lambda \exp \left( -\frac{\Theta}{\theta} \right) \left[ a - \frac{1}{\exp(\Delta/\theta) + 1} \right], \quad (34)$$

where  $\Lambda = L_f/(\tau_R U_f)$  is an eigenvalue of the stationary problem and the designation  $J$  corresponds to the ratio of Zeeman and thermal energies,

$$J = \frac{f Q \Theta_p^\alpha}{A k_B T_f^{\alpha+1}}. \quad (35)$$

It can be shown that the parameter  $J$  is almost a constant,  $J \approx 1/(\alpha+1)$ . We also introduce the thermal flux,  $\psi = \theta^{\alpha-\beta} \partial \theta / \partial \xi$ , so that the stationary deflagration is described by the system of equations

$$\begin{aligned} \frac{\partial \psi}{\partial \xi} &= \theta^\beta \psi - J \Lambda a \exp \left( -\frac{\Theta}{\theta} \right), \\ \frac{\partial \theta}{\partial \xi} &= \theta^{\beta-\alpha} \psi, \\ \frac{\partial a}{\partial \xi} &= -\Lambda a \exp \left( -\frac{\Theta}{\theta} \right). \end{aligned} \quad (36)$$

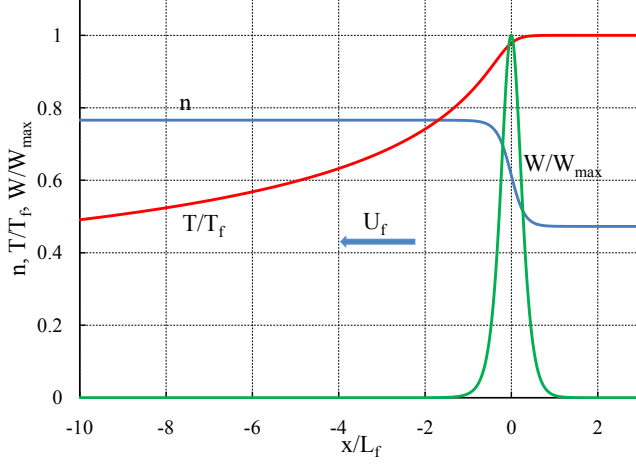


FIG. 3: Stationary profiles of concentration, temperature and energy release. The plot parameters are  $E_a/T_f = 30$ ,  $\beta = 3$ ,  $\theta_0 = 0.2$

Typical profiles of scaled concentration, temperature and energy release

$$W = \Lambda \exp\left(-\frac{\Theta}{\theta}\right) \left[ a - \left( \exp\left(\frac{\Delta}{\theta}\right) + 1 \right)^{-1} \right] \quad (37)$$

are depicted in Fig. 3 for the magnetic deflagration propagating to the left with  $\beta = 3$ . In Fig. 3, the scaled activation energy is taken rather high,  $\Theta = 30$ , with the initial temperature  $\theta_0 = 0.2$ . The front velocity is determined by the eigenvalue of the problem  $\Lambda$  in Eq. (36), which was computed numerically using the shooting method similar to<sup>31</sup>. We can see in Fig. 3 that final number of molecules in the metastable state behind the deflagration front is different from zero  $n_f = 0.47$ , which indicates that burning is incomplete. Initial number of molecules in the metastable state is different from unity too,  $n_0 = 0.77$ , due to the non-zero temperature ahead of the front before switching of the magnetic field, see Eq. (4). Figure 3 shows also that the total thickness of the deflagration front is much larger than  $L_f$ . This difference in the characteristic length scales should be attributed, first of all, to the temperature dependence of thermal conduction. Still, even in the case of constant thermal conduction typically used in combustion problems, the effective flame thickness is almost order-of-magnitude larger than the conventional definition for  $L_f$ , e.g. see<sup>32</sup>. The asymptotic temperature behavior ahead of the front is described by a single differential equation, derived from Eq. (33), assuming that  $\exp(-\Theta/\theta) \ll 1$  in the cold matter

$$\frac{\partial \theta}{\partial \xi} + \frac{\theta^{\beta-\alpha}}{\alpha+1} (\theta_0^{\alpha+1} - \theta^{\alpha+1}) = 0. \quad (38)$$

Equation (38) determines variations of the length scale in the temperature profile.

Now we consider stability of the magnetic deflagration. We investigate dynamics of small perturbations of the stationary solution, so that all variables may be presented as  $\varphi = \varphi_0 +$

$\tilde{\varphi} \exp(\gamma \tau)$ . Then the perturbed system (36) is

$$\begin{aligned} \frac{\partial \tilde{\psi}}{\partial \xi} &= \theta^\beta \tilde{\psi} + \left( \theta^\alpha \sigma + \beta \theta^{\beta-1} \psi - JG \right) \tilde{\theta} - J\Lambda \exp\left(-\frac{\Theta}{\theta}\right) \tilde{a}, \\ \frac{\partial \tilde{\theta}}{\partial \xi} &= \theta^{\beta-\alpha} \tilde{\psi} + (\beta - \alpha) \theta^{\beta-\alpha-1} \psi \tilde{\theta}, \\ \frac{\partial \tilde{a}}{\partial \xi} &= -G \tilde{\theta} - \left( \sigma + \Lambda \exp\left(-\frac{\Theta}{\theta}\right) \right) \tilde{a}, \end{aligned} \quad (39)$$

where the designation

$$G = \Lambda \exp\left(-\frac{\Theta}{\theta}\right) \frac{1}{\theta^2} \left[ \Theta a - \left( \Theta - \frac{\Delta}{\exp(\Delta/\theta) + 1} \right) \frac{1}{\exp(\Delta/\theta) + 1} \right]$$

has been introduced for brevity. Parameter  $\gamma$  stands for the scaled instability growth rate,  $\gamma = \sigma L_f / U_f$ . In order to specify boundary conditions for the numerical solution, we find the decaying perturbation modes in the uniform regions,  $\tilde{\varphi} \propto \tilde{\varphi} \exp(\mu \xi)$ . The system (39) involves three modes in the uniform regions: one in the hot matter with  $\mu < 0$ ,  $\xi \rightarrow +\infty$ , and two in the cold matter with  $\mu > 0$ ,  $\xi \rightarrow -\infty$ . We integrate the system (39) numerically three times corresponding to the three perturbation modes: two times from the left (cold) side and one from the right (hot) side. At some point, e.g., at the maximum of the energy release, the solutions form a matrix, with the determinant depending on the instability growth rate,  $\gamma$ . The condition of zero matrix determinant specifies the growth rate  $\gamma$  as an eigenvalue of the system (39). This method has been applied successfully in studies of different hydrodynamic instabilities, e.g. the Rayleigh-Taylor instability and the Darrieus-Landau instability of combustion and laser ablation, as well as for other plasma instabilities<sup>31,33-35</sup>.

## V. RESULTS AND DISCUSSIONS

Numerical solution to the stability problem is shown in Fig. 4 for different values of the scaled activation energy proportional to Zeldovich number as  $E_a/T_f = 4Z$  for a 3D problem; other deflagration parameters are the same as used in Fig. 3. As we can see in Fig. 4, planar stationary magnetic deflagration is unstable at sufficiently large values of the scaled activation energy; the stability limit was calculated as  $E_a/T_f = 28.2$ . The instability domain consists of two parts separated by the bifurcation point at  $E_a/T_f = 33.2$ . Most of the domain (to the right of the bifurcation point) corresponds to purely real instability growth rate  $\sigma > 0$  with two branches describing the fast and slow perturbation modes (shown by the solid lines). The instability growth rate of the fast mode increases with the scaled activation energy without any limit. The analytical model, Eq. (31), predicts the asymptotic increase of the growth rate for the fast mode as  $\sigma \propto (E_a/T_f)^2$  for  $E_a/T_f \rightarrow \infty$ . The growth rate of the slow mode decreases with the scaled activation energy. For this reason it is expected that the slow mode plays a noticeable role only close to the bifurcation point, where the growth rates of the fast and slow modes are



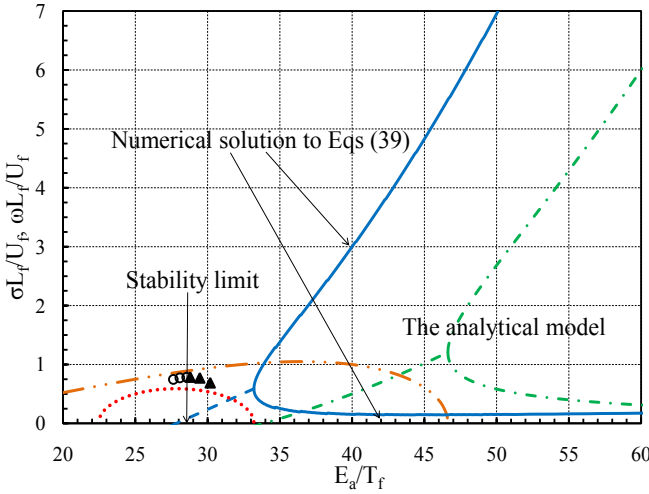


FIG. 4: The instability growth rate  $\sigma$  and the perturbation frequency  $\omega$  versus the scaled activation energy calculated for the same parameters as in Fig. 3. Solid lines show the domain of zero frequency; the dashed and dotted lines correspond to the regimes when perturbations have both real (growth rate,  $\sigma$ ) and imaginary part (frequency,  $\omega$ ) in the problem eigenvalue. The dash-dotted lines present the analytical model Eq. (28). The markers show results of the direct numerical simulations: empty circles stand for stable region and filled triangles represent the unstable pulsating regime of the deflagration.

comparable. In a small part of the instability domain, for intermediate values of the scaled activation energy in between the stability limit and the bifurcation point,  $28.2 < E_a/T_f < 33.2$ , the instability growth rate is complex with the real part,  $\sigma > 0$  (dashed line), and imaginary part,  $\omega$  (dotted line). Although this part of the instability domain is rather small, it indicates the physical outcome of the instability at the nonlinear stage. Because of the non-zero frequency,  $\omega \neq 0$ , it is natural to expect that the instability leads to a pulsating regime of magnetic deflagration at the nonlinear stage. The analytical solution, Eq. (31), obtained within the model of a thin transition zone (dashed-dotted lines) shows qualitatively the same stability properties of magnetic deflagration as the numerical solution. Still, we observe minor quantitative difference between the analytical model and the numerical solution. According to the analytical model, the stability limit and the bifurcation point are expected at  $E_a/T_f = 34.0$  and  $E_a/T_f = 46.8$ , which differ by approximately 20-30% from the respective numerical values. The limited accuracy of the analytical model is due to the simplifying approximations of 1) a constant coefficient of energy diffusion and 2) an infinitely thin zone of energy release. In particular, the shortcomings of the discontinuity model have been discussed in [24,25] in the context of solid propellant combustion.

The numerical solution to the stability problem indicates the experimental parameters required to observe the unstable non-stationary regime of magnetic deflagration. We plot the stability diagram in Fig. 5 in  $f - H_z$  coordinates using Eq. (17); the shading represents absolute value of the instability growth rate. The dashed white line in Fig. 5 corresponds to the critical value of the Zeldovich number (the stability limit)

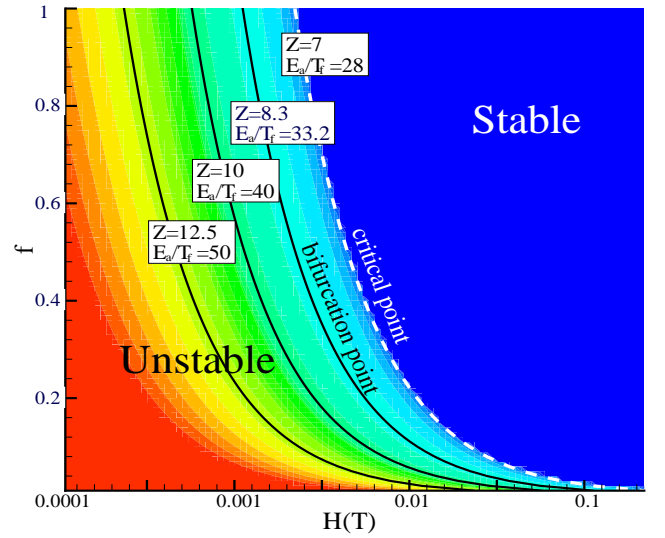


FIG. 5: The stability limit (dashed line) of the magnetic deflagration in coordinates of the dilution factor  $f$  and the magnetic field  $H$ . The shading shows the instability growth rate. Other solid lines correspond to the respective constant values of the Zeldovich number.

obtained numerically. Magnetic deflagration propagates stationary in the parameter domain to the right of the stability limit, in the region of a high magnetic field. To the left of the critical curve, for a low magnetic field, the stationary magnetic deflagration is unstable, and we expect a pulsating regime of the deflagration front. Particularly, in the case of  $\text{Mn}_{12}$  with the dilution level  $f = 1/3$  one should expect the instability for the magnetic fields below  $10^{-2}\text{T}$ , which is possible to achieve experimentally.

In order to understand front dynamics at the nonlinear stage of the instability, we perform direct numerical simulation of Eqs. (33)-(34). In our simulations we use the method of finite difference for the spatial derivatives and the common fourth order Runge-Kutta method for the time step integration. Since the front structure is 1D, then we were able to obtain fine front resolution together within acceptable time of computational runs. The results of our simulations, i.e. evolution of the magnetic deflagration speed, are shown in Fig. 6 for different values of the scaled activation energy. Figures 6 a, b demonstrate front behavior close to the stability limit in the stable (a) and unstable (b) parameter domain. In the first case with  $E_a/T_f = 28.55$ , the velocity perturbation oscillates and decays in time, which implies a negative instability growth rate. On the contrary, in Fig. 6b with  $E_a/T_f = 28.8$ , the amplitude of velocity oscillations grows in time, which corresponds to the instability onset. The markers in Fig. 4 show the oscillation frequency of the magnetic deflagration obtained in direct numerical simulations with empty circles and filled triangles standing for the stable and unstable regimes, respectively. As we can see, the direct numerical simulations are in a good agreement with the solution to the eigenvalue problem, which concerns both the stability limits and the oscillation frequency. Still, the instability is rather weak in Fig. 6 b with the oscillations described well by the sine function. The nonlinear

effects become noticeable for higher values of the scaled activation energy with sharp peaks and smooth troughs in the oscillations as presented in Fig. 6c for  $E_a/T_f = 30.2$ . The simulations explain the physical mechanism of the obtained instability. Magnetic deflagration propagates due to two effects: release of the Zeeman energy in a thin transition zone and transfer of the energy to the cold layers (preheating) due to thermal conduction. In a stationary regime of magnetic deflagration, these two processes work at the same rate and balance each other. However, at high values of the activation energy, the rate of energy release is too sensitive to temperature in the transition zone. Small temperature perturbations may increase the “burning” rate considerably, which makes the transition zone sweep fast over the preheated matter until it comes to cold regions and stops waiting for a new portion of cold matter to be preheated. As soon as it happens, next pulsation of the front takes place.

It is interesting that the three figures 6 a, b and c demonstrate three qualitatively different regimes of magnetic deflagration, though the activation energy changes only within 5% from plot (a) to plot (c). In Fig 6 d we take the activation energy  $E_a/T_f = 33.8$  close to the bifurcation point and see a complicated front behavior at the onset of the velocity pulsations. Presumably, the complicated behavior happens because of two unstable modes with close instability growth rates at the vicinity of the bifurcation point. Still, after an initial transition period, the front pulsations resemble those of Fig. 6 c. Finally, taking the activation energy noticeably larger than the bifurcation point,  $E_a/T_f = 40$ , we observe even more pronounced nonlinear features in the front oscillations with even sharper peaks of large amplitude, shown in Fig. 6e. The obtained results are qualitatively similar to the pulsation instability of solid propellant combustion studied in, e.g., [21,23].

As we have shown, the scaled activation energy (or the Zel'dovich number) is the main parameter, which controls 1D stability properties of magnetic deflagration. Still, the problem involves other parameters as well, namely, power exponents  $\alpha$  and  $\beta$  in the heat capacity and thermal conduction, respectively, and the scaled initial temperature of the system  $\theta_0$ . Figure 7 shows the instability growth rate for different types of thermal conduction (different values of the power exponent  $\beta$ ,  $13/3 > \beta > 0$ ). As we can see, a particular type of the thermal conduction influences the temperature profile in the stationary magnetic deflagration noticeably in agreement with Eq. (34), see the insert of Fig. 7. At the same time, the stationary profiles of concentration and energy release remain the same for different values of the  $\beta$ -factor. The power exponent  $\beta$  determines the total length scale of the deflagration front in the cold region. However, even considerable variations of  $\beta$  modify the instability growth rate only slightly: the stability limit changes only by 5% from  $E_a/T_f = 27.9$  to  $E_a/T_f = 29.4$ ; the bifurcation point changes within 15% from  $E_a/T_f = 32$  to  $E_a/T_f = 37$ . This result demonstrates that the perturbation modes are strongly localized around the zone of energy release within the length scale about  $L_f$  as we explained in Sec. III. For this reason, considerable modifications of the temperature profile in the far zone on the length scales much larger than  $L_f$  due to variations of  $\beta$  produce a minor effect on the

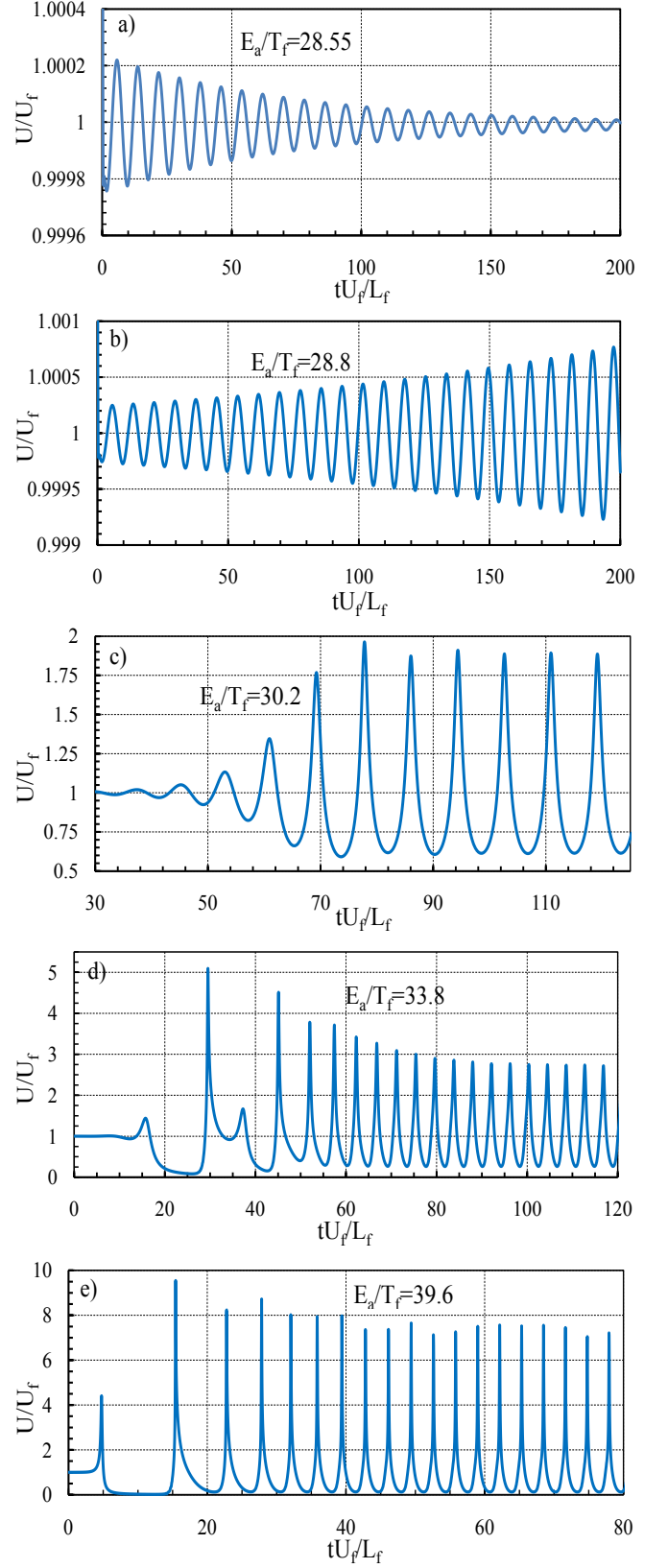


FIG. 6: Deflagration speed versus time for different values of the scaled activation energy  $E_a/T_f = 28.55$ ; 28.8; 30.2; 33.8; 39.6 for plots (a) - (e), respectively.



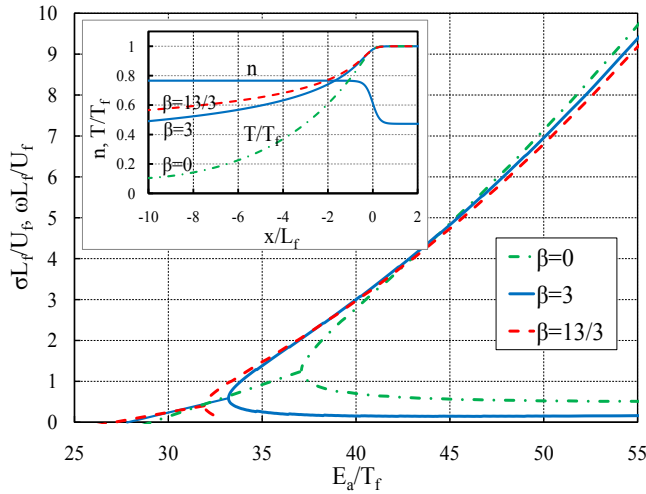


FIG. 7: The instability growth rate  $\sigma$  versus the scaled activation energy calculated for different values of the power exponent  $\beta$ . Other parameters are  $\alpha = 3$ ,  $\theta_0 = 0.2$ . The inset presents the respective temperature profiles for  $E_a/T_f = 30$  and  $\beta = 0; 3$ .

stability properties. Influence of the initial temperature on the instability development is even weaker. In particular, changing the scaled initial temperature from  $\theta_0 = 0.2$  to  $\theta_0 = 0.5$ , we find modifications of the stability properties by about 5%.

Unlike  $\beta$  and  $\theta_0$ , the system dimension  $\alpha$  (and the power exponent in phonon heat capacity) influences the critical values of the scaled activation energy  $E_a/T_f$  considerably since it is involved in the Zeldovich number according to Eq. (15). At the same time, the critical Zeldovich number changes slightly for different values of  $\alpha$ . For example, we obtain the scaled activation number  $E_a/T_f = 13.7$  and the critical Zel-

dovich number  $Z = 6.8$  for  $\alpha = 1$ , which may be compared to  $E_a/T_f = 28.2$  and  $Z = 7.0$  found for  $\alpha = 3$ . Besides, one may also expect different types of heat capacity apart from the phonon type, which may modify the power law Eq. (8) and the respective deflagration stability properties<sup>9,36,37</sup>.

## VI. SUMMARY

In this paper we have obtained 1D instability of magnetic deflagration in a medium of molecular magnets. The main parameter of the problem is the Zeldovich number, which represents the activation energy of the system (in temperature units) scaled by the temperature at the deflagration front with a numerical factor depending on the type of heat capacity. We have demonstrated that the deflagration front becomes unstable when the Zeldovich number exceeds a certain critical value  $Z \approx 7$ . We have obtained the analytical scaling for the instability parameters at the linear stage within the model of an infinitely thin zone of Zeeman energy release. We have also solved the eigenvalue stability problem numerically taking into account the internal structure of the deflagration front. The numerical solution determines the experimental parameters necessary to observe the instability. Besides, we have performed direct numerical simulations, which demonstrated that the instability leads to a pulsating regime of magnetic deflagration at the nonlinear stage.

## Acknowledgments

This work was supported by the Swedish Research Council and by the Kempe Foundation.

- <sup>1</sup> D. Gatteschi and R. Sessoli, *Angew. Chem., Int. Ed.* **42**, 268 (2003).
- <sup>2</sup> E. del Barco, A. D. Kent, S. Hill, J. M. North, N. S. Dalal, E. Rumberger, D. N. Hendrikson, N. Chakov, and G. Christou, *J. Low Temp. Phys.* **140**, 119 (2005).
- <sup>3</sup> M. N. Leuenberger and D. Loss, *Nature (London)* **410**, 789 (2001).
- <sup>4</sup> J. Tejada, E. M. Chudnovsky, E. del Barco, J. M. Hernandez, and T. P. Spiller, *Nanotechnology* **12**, 181 (2001).
- <sup>5</sup> R. Sessoli, D. Gatteschi, A. Caneschi, and M. A. Novak, *Nature (London)* **365**, 141 (1993).
- <sup>6</sup> C. Paulsen *et al.*, *J. Magn. Magn. Mater.* **140**, 1891 (1995).
- <sup>7</sup> J. R. Friedman, M. P. Sarachik, J. Tejada, and R. Ziolo, *Phys. Rev. Lett.* **76**, 3830 (1996).
- <sup>8</sup> L. Thomas, F. Lioni, R. Ballou, D. Gatteschi, R. Sessoli, and B. Barbara, *Nature (London)* **383**, 145 (1996).
- <sup>9</sup> F. Fominaya, J. Villain, P. Gandit, J. Chaussy, and A. Caneschi, *Phys. Rev. Lett.* **79**, 1126 (1997).
- <sup>10</sup> E. del Barco, J. M. Hernandez, M. Sales, J. Tejada, H. Rakoto, J. M. Broto, and E. M. Chudnovsky, *Phys. Rev. B* **60**, 11898 (1999).
- <sup>11</sup> Y. Suzuki, M. P. Sarachik, E. M. Chudnovsky, S. McHugh, R. Gonzalez-Rubio, N. Avraham, Y. Myasoedov, E. Zeldov, H. Shtrikman, N. E. Chakov, and G. Christou, *Phys. Rev. Lett.* **95**, 147201 (2005).
- <sup>12</sup> D. A. Garanin and E. M. Chudnovsky, *Phys. Rev. B* **76**, 054410 (2007).
- <sup>13</sup> A. Hernandez-Minguez, J. M. Hernandez, F. Macia, A. Garcia-Santiago, J. Tejada, and P. V. Santos, *Phys. Rev. Lett.* **95**, 217205 (2005).
- <sup>14</sup> S. McHugh, R. Jaafar, M. P. Sarachik, Y. Myasoedov, A. Finkler, H. Shtrikman, E. Zeldov, R. Bagai, and G. Christou, *Phys. Rev. B* **76**, 172410 (2007).
- <sup>15</sup> A. Hernandez-Minguez, F. Macia, J. M. Hernandez, J. Tejada, and P. V. Santos, *J. Magn. Magn. Mater.* **320**, 1457 (2008).
- <sup>16</sup> D. Villuendas, D. Gheorghe, A. Hernandez-Minguez, F. Macia, J. M. Hernandez, J. Tejada, R. J. Wijngaarden, *EPL (Europhysics Letters)* **84**, 67010 (2008).
- <sup>17</sup> S. McHugh, B. Wen, X. Ma, M. P. Sarachik, Y. Myasoedov, E. Zeldov, R. Bagai, and G. Christou, *Phys. Rev. B* **79**, 174413 (2009).
- <sup>18</sup> W. Decelle, J. Vanacken, V. V. Moshchalkov, J. Tejada, J. M. Hernandez, and F. Macia, *Phys. Rev. Lett.* **102**, 027203 (2009).
- <sup>19</sup> Ya. B. Zeldovich, G. I. Barenblatt, V. B. Librovich, G. M. Makhviladze, *The Mathematical Theory of Combustion and Ex-*

- plosion*, Consultants Bureau, New York (1985).
- <sup>20</sup> S. Velez, J. M. Hernandez, A. Fernandez, F. Macia, C. Magen, P. A. Algarabel, J. Tejada, and E. M. Chudnovsky, *Phys. Rev. B* **81**, 064437 (2010).
  - <sup>21</sup> K. G. Shkadinsky, B. I. Khaikin, and A. G. Merzhanov, *Combust. Expl. Shock Waves* **7**, 15 (1971).
  - <sup>22</sup> B. J. Matkovsky and G. I. Sivashinsky, *SIAM J. Appl. Math.* **35**, 465 (1978).
  - <sup>23</sup> M. Frankel, V. Roytburd, and G. Sivashinsky, *SIAM J. Appl. Math.* **54**, 1101, (1994).
  - <sup>24</sup> V. V. Bychkov, M. A. Liberman, *Phys. Rev. Lett.* **73**, 1998 (1994).
  - <sup>25</sup> V. V. Bychkov, M. A. Liberman, *Phys. Rep.* **325**, 115 (2000).
  - <sup>26</sup> P. Artus, C. Boskovic, J. Yoo, W. E. Streib, L. C. Brunel, D. N. Hendrickson, and G. Christou, *Inorg. Chem.* **40**, 4199 (2001).
  - <sup>27</sup> C. Schlegel, J. van Slageren, M. Manoli, E. K. Brechin, M. Dressel, *Polyhedron* **28**, 1834 (2009).
  - <sup>28</sup> T. L. Makarova, V. S. Zagaynova, and N. G. Spitsina, *Phys. Status Solidi B* **247**, 3018 (2010).
  - <sup>29</sup> C. Kittel, *Quantum Theory of Solids*, Wiley, New York, (1963).
  - <sup>30</sup> D. A. Garanin and V. S. Lutovinov, *Ann. Phys. (N. Y.)* **218**, 293 (1992).
  - <sup>31</sup> M. Modestov, V. Bychkov, D. Valiev, and M. Marklund, *Phys. Rev. E* **80**, 046403 (2009).
  - <sup>32</sup> V. Akkerman, V. Bychkov, A. Petchenko, L.E. Eriksson, *Combust. Flame* **145**, 675 (2006).
  - <sup>33</sup> O. Travnikov, V. Bychkov, and M. Liberman, *Phys. Fluids* **11**, 2657 (1999).
  - <sup>34</sup> M. Modestov, V. Bychkov, and M. Marklund, *Phys. Plasmas* **16**, 032106 (2009).
  - <sup>35</sup> V. Bychkov, M. Modestov, and M. Marklund, *Phys. Plasmas* **17**, 112107 (2010).
  - <sup>36</sup> A. M. Gomes, M. A. Novak, R. Sessoli, A. Caneschi, and D. Gatteschi, *Phys. Rev. B* **57**, 5021 (1998).
  - <sup>37</sup> F. Fominaya, J. Villain, T. Fournier, P. Gandit, J. Chaussy, A. Fort, and A. Caneschi, *Phys. Rev. B* **59**, 519 (1999).